Simultaneous Two-Photon Excitation of Photofrin® in Relation to Photodynamic Therapy [‡]

Aliaksandr Karotki, Mamta Khurana, James R. Lepock, Brian C. Wilson*

Division of Biophysics and Bioimaging, Ontario Cancer Institute/University of Toronto, Toronto, ON, Canada.

* Corresponding author

Ontario Cancer Institute/University of Toronto

610 University Ave, Rm 7-417

Toronto, ON M5G2M9

Canada

Phone: 416 946 2952

Fax: 416 946 6529

e-mail: wilson@uhnres.utoronto.ca

Keywords: two-photon absorption, photodynamic therapy, Photofrin, two-photon cross section, endothelium.

Abbreviations: AMD, age related macular degeneration; CW, continuous wave; fs, femtosecond; FWHM, full width at half maximum; PDT, photodynamic therapy; 1-γ, single-photon; 3D, three-dimensional; 2-γ, two-photon.

[‡] Published in the journal website (www.ASPjournal.com) on xx-xxx-xxx.

ABSTRACT

Photodynamic therapy (PDT), the use of light-activated drugs (photosensitizers), is an emerging treatment modality for tumors as well as various non-oncologic conditions. Single-photon (1-γ) PDT is limited by low specificity of the photosensitizer, leading to the damage to healthy tissue adjacent to the diseased target tissue. One solution is to use simultaneous two-photon (2-γ) excitation with ultrafast pulses of near-infrared light. Due to the non-linear interaction mechanism, 2-γ excitation with a focused beam is localized in three dimensions, allowing treatment volumes on the order of femtoliters. We propose that this will be valuable in PDT of age-related macular degeneration (AMD), which causes blindness due to abnormal choroidal neovasculature and which is currently treated by 1-γ PDT. Here, Photofrin® has been used as the photosensitizer to demonstrate proof-of-principle of 2-γ killing of vascular endothelial cells *in vitro*. The 2-γ absorption properties of Photofrin were investigated in the 750-900 nm excitation wavelength range. It was shown that 2-γ excitation dominates over 1-γ excitation above 800 nm. The 2-γ absorption spectrum of Photofrin in the 800 – 900 nm excitation wavelength range was measured. The 2-γ cross section decreased from about 10 GM (1 GM = 10^{-50} cm^4s/photon) at 800 nm to 5 GM at 900 nm. Adherent YPEN-1 endothelial cells were then incubated with Photofrin for 24 h and then treated by PDT at 850 nm where the 1-γ contribution was negligible. Cell death was monitored using 2-γ scanning laser microscopy. The light doses required for killing were high (6300 Jcm^{-2} for ~ 50% killing), but 2-γ cytotoxicity was unequivocally demonstrated. While Photofrin is, per se, not a good choice for 2-γ PDT due to its low 2-γ cross section, this work provides baseline data to guide the

development of novel photosensitizers with much higher 2-γ cross-sections (>100 GM), which will be required for 2-γ PDT of AMD (and other conditions) to be clinically practical.

INTRODUCTION

PDT is gaining acceptance as treatment for tumors, as well as some non-tumor conditions (1,2). It employs photosensitizers that produce cytotoxic reactive oxygen species upon excitation with light, most commonly singlet oxygen ($^1O_2$), as illustrated in Figure 1a. PDT is a minimally-invasive technique that avoids many of the side-effects typical for radiation and chemotherapy, since the drug and light by themselves are not cytotoxic. In particular, in the past few years, PDT has become the treatment of choice for neovascular AMD, in which there is abnormal growth of choroidal neovasculature that eventually obscures central vision, leading to blindness (3). PDT using the photosensitizer benzoporphyrin-mA (Visudyne®, QLT Inc, BC, Canada) is used to target the neovasculature by delivering the light while the photosensitizer is still primarily in the circulation, with the continuous wave (CW) light from a diode laser delivered to a spot of a few mm diameter via a fundus camera. However, one of the main limitations of current PDT is the relatively low specificity of the photosensitizers for diseased tissues/cells (4). Partial selectivity is achieved by directing the excitation light to the desired treatment area. Nevertheless adjacent healthy tissue may also be damaged (5,6), so that a large effort is directed to the development of new photosensitizers with higher disease affinity.

To date, all clinical PDT, including that for AMD, has used 1-γ excitation of the photosensitizer, in which the singlet-state of the drug is generated upon absorption of one photon, usually in the visible range. In the case of $^1O_2$-dependent PDT, this singlet excited state then undergoes intersystem crossing to a long-lived triplet, which then generates $^1O_2$ by energy transfer to the triplet ground state of molecular oxygen in the tissue. An alternative is to activate the photosensitizer by the simultaneous absorption of two, long-wavelength photons (Figure 1a).

Since the probability of this 2-γ process depends on the *square* of the local light intensity, the photosensitizer activation is more localized than 1-γ activation, thereby improving the target specificity. As illustrated in Figure 1b, 2-γ PDT using a focused light beam is effectively localized not only in the transverse plane but also along the laser beam. This 3D localization effect has been used successfully in 2-γ microscopy for more than a decade (7,8).

The probability of 2-γ excitation is usually much lower than that of 1-γ excitation. Since the probability of 2-γ absorption is proportional to the product of the 2-γ cross-section and the square of the local light intensity, it is necessary to use as short a laser pulse as possible to give the highest instantaneous power density, preferably in a diffraction-limited focal spot at the target. In practice, as discussed below, pulses of ~100 fs are probably optimal. The use of near-infrared photons is also desirable, since these have greater penetration through tissues (9) and can be selected to lie beyond the longest 1-γ absorption band. The latter is particularly important for 2-γ PDT of AMD, since the objective is to minimize any PDT effect outside the focal volume.

To date there have been several reports dealing with 2-γ PDT (see for example (10-16)). In a number of studies (10-12,14), the biological effects of 2-γ PDT using known 1-γ photosensitizers have been determined, but without knowledge of the 2-γ spectra and cross sections. Hence, although the principle of 2-γ cytotoxicity has been demonstrated, it is difficult to compare these results, either with each other or with the corresponding 1-γ efficacy of the photosensitizers. Other reports (13,15,16) have been aimed at synthesis and characterization of the photophysical properties of new photosensitizers with high 2-γ cross-sections. However, their efficiency in biological systems is unknown.

The objectives of the present study were to establish quantitatively the 2-γ spectrum and

cross-section for Photofrin, selected as the archetypal 1-γ photosensitizer (1) that is used widely in both pre-clinical and clinical studies, and to measure its 2-γ photocytotoxicity in vascular endothelial cells as an *in vitro* model relevant to PDT of neovascular diseases such as AMD. This will allow its use as a reference for new photosensitizers developed specifically for 2-γ PDT as well as will provide data to determine 2-γ cross sections required for efficient 2-γ PDT. In addition, if Photofrin does possess high enough cross sections for efficient 2-γ activation, then it may be used in 2-γ PDT with the advantage of there being a large body of knowledge of its photobiological effects.

This paper describes the use of a 2-γ laser scanning microscope for measurements of the 2-γ spectra and cross section of Photofrin and demonstrates 2-γ PDT effect of Photofrin on vascular endothelial cells YPEN-1.

MATERIALS AND METHODS

Materials. Lucifer Yellow CH (ammonium salt) and SYTOX Orange were acquired from Molecular Probes/Invitrogen (Burlington, ON, Canada), Hoechst 33258 was acquired from Terochem Laboratories (Mississauga, ON, Canada), Rhodamine B was acquired from Fisher Scientific (Ottawa, ON, Canada) and Photofrin® from Axcan Pharma (Montreal, QC, Canada).

Two-photon microscope. All the 2-γ experiments were performed using a confocal scanning microscope (LSM 510 META NLO: Carl Zeiss, Ltd, Toronto, ON, Canada) coupled to a femtosecond (fs) Ti:Sapphire laser (Chameleon: Coherent, Santa Clara, CA, USA) the wavelength of which could be selected in the range 720 – 930 nm, with a pulse duration at the sample position of 300 fs and a pulse repetition rate of 90 MHz. 1-γ excitation was performed using an argon-ion laser operating at 488 nm and also coupled to the microscope. A simplified diagram of the excitation and fluorescence collection pathways of the microscope is presented in Figure 2. During 2-γ spectral and cross section measurements the average optical power at the sample position was varied in the range 10-30 mW for the Ti:sapphire laser and 10-50 μW for the argon-ion laser to confirm the 2-γ and 1-γ power dependence, respectively. For 2-γ PDT experiments the average power of the Ti:sapphire laser was kept at 10 mW. The advantage of using the microscope was that it allowed direct imaging of the cells pre, during and post irradiation.

For 2-γ in vitro studies (see below) a 40× water immersion objective with a numerical aperture of 1.2 was used. The monolayer cell culture was scanned in a uniform raster pattern by the focused laser light over a 512×512 pixel area of 230 μm × 230 μm. The pixel dwell time was 1.6 μs. The de-scanned fluorescence from the sample was directed to the photomultiplier through several filters that cut off the scattered excitation laser light. For the 2-γ absorption spectrum and

cross section measurements, fluorescence from the photosensitizer in bulk solution was detected using a 10×, 0.5 NA dry objective. The scanned area in this case was 921 μm × 921 μm (512 × 512 pixels). For all the quantitative measurements we confirmed that the photodetector response was linear over the range of detected fluorescence intensities.

Two-photon absorption spectrum. Since the probability of 2-γ excitation is small, the absorption spectrum is usually measured by detecting the 2-γ excited fluorescence rather than directly by light attenuation through the sample. The fluorescence intensity is proportional to the product of the 2-γ absorption coefficient and the fluorescence quantum yield. By changing the excitation wavelength and assuming that the fluorescence quantum yield does not change with wavelength, one can build the relative 2-γ spectral profile. These measurements are non trivial, since the pulse energy, pulse duration and pulse shape all influence the 2-γ excitation efficiency. The fs laser in the microscope system is purposely designed as a user-friendly 'black box' for standard 2-γ imaging and allows only very limited control over the output parameters. It is possible to measure these output pulse characteristics and then modify them to some extent, for example using neutral-density filters to change the pulse energy. Alternatively, it is possible to use the unmodified laser pulses and then to normalize the 2-γ fluorescence signal to the excitation photon flux (quadratic dependence) and pulse duration (inverse linear dependence) at a specific selected wavelength. However, both of these approaches require accurate knowledge of the fs laser pulses properties that is not easily available, or modification of which complicates the experimental setup. Hence, we opted instead to measure the 2-γ spectrum relative to that of a reference compound for which the spectrum is well established over the desired wavelength range, so that knowledge of the fs pulse characteristics is not required. These measurements were performed using 4-well plates, each containing the photosensitizer, reference compound or their

respective solvents. The last allows subtraction of the contribution of background signal from the solvents. The relative 2-γ spectrum of the photosensitizer, $S(\lambda)$, was then calculated from:

$$S(\lambda) = \frac{F(\lambda) - F_s(\lambda)}{F_r(\lambda) - F_{s,r}(\lambda)} S_r(\lambda), \quad (1)$$

where $F(\lambda)$, $F_s(\lambda)$, $F_r(\lambda)$ and $F_{s,r}(\lambda)$ are 2-γ fluorescence signals of the photosensitizer, photosensitizer solvent, reference compound and reference solvent, respectively, and $S_r(\lambda)$ is the known 2-γ reference spectrum. Note that $S(\lambda)$ gives only the shape of the 2-γ absorption spectrum, not the absolute values, even if the reference spectrum, $S_r(\lambda)$, is known in absolute units because factors such as the detector sensitivity, filters transmission and fluorescence quantum yields are different for the reference and studied compounds.

Lucifer Yellow dissolved in water, for which the 2-γ spectrum is known, was used as the reference compound (17). The 2-γ absorption spectrum of Lucifer Yellow in the 750-950 nm range is the same as 1-γ absorption spectrum at half the wavelength measured by us (data not shown). This is in accordance with the fact that, for molecules without a center of inversion, both 1-γ and 2-γ transitions are allowed between the same energy levels. This makes Lucifer Yellow particularly convenient as a reference because the much smoother profile of the 1-γ absorption band around 430 nm can be used as the reference, S_r, in equation (1) by simply doubling each wavelength. To confirm the validity of this approach, we used it to measure the 2-γ spectrum of Rhodamine B in methanol. As shown in Figure 3, this is in good agreement with the published spectrum that was measured directly (17). All the 2-γ absorption spectra and cross section measurements were done using following concentrations: Lucifer Yellow ~ 10^{-4} M, Rhodamine B ~ 10^{-5} M, Photofrin = 100 μg/ml.

Two-photon cross section. In order to obtain the absolute 2-γ cross section of Photofrin,

we used a technique comparing its 1-γ and 2-γ excited fluorescence. This method was first proposed by Galanin and Chizhikova (18) and later used with some modifications in a number of studies (17-22). The advantage is that a reference chromophore is not required. We have closely followed the method described in (17), as follows.

In the irradiation geometry used, the 2-γ fluorescence is concentrated around the focal point of the scanning fs laser beam in the microscope. The length of the excitation volume along the laser beam, ω, can be estimated (8) as:

$$\omega = \sqrt{2}\,\frac{0.532\lambda}{n - \sqrt{n^2 - NA^2}}, \tag{2}$$

where λ is the excitation wavelength and n is the refractive index of the objective immersion medium (in our case n = 1). For the 10×, 0.5NA objective ω~5 μm. 2-γ excitation was done in 4-well plates with a solution depth of several millimeters, so that the depth does not affect the number of 2-γ excited molecules. Hence, the number of 2-γ absorbed photons, $N_2(t)$, is given by (17):

$$N_2(t) = \frac{8c\sigma_2 g n \langle P_2(t)\rangle^2}{\lambda_2 f \tau \pi}, \tag{3}$$

where c is the chromophore concentration, σ_2 is the 2-γ cross section [cm^{4}s/photon], g is a numerical factor that depends on the laser pulse shape (we assume Gaussian pulse shape for which g = 0.664), and $\langle P_2(t)\rangle$, λ_2, f, and τ are the average power [photons/s], wavelength [cm], repetition rate [Hz], and pulse duration [s] (FWHM) of the fs laser light. The detected 2-γ fluorescence signal, $F_2(t)$, then is:

$$F_2(t) = \frac{1}{2}\Phi\eta N_2(t), \tag{4}$$

where the factor of ½ means that two photons are required to excite one molecule, Φ is the fluorescence quantum yield and η is the collection efficiency of the microscope optics and detector. As mentioned above, an argon-ion laser working at 488 nm was used for 1-γ excitation. Since 1-γ fluorescence is excited throughout the sample depth, the collection efficiencies for 1-γ and 2-γ fluorescence in a thick sample are different. Hence, we used a demountable cell with 10 μm sample thickness for the 1-γ measurements (17). Thereby, fluorescence is excited only around the focal point of the objective and the fluorescence collection efficiency, η, is the same as for 2-γ excitation. Note that the pinhole in front of the microscope photodetector was fully open during 1-γ and 2-γ excitation (diameter 1mm), so that it did not have any effect on the detection efficiency. The number of 1-γ absorbed photons, $N_1(t)$, is:

$$N_1(t) = \langle P_1 \rangle (1 - \exp[-\sigma_1 cL]) \approx \langle P_1 \rangle \sigma_1 cL \,, \tag{5}$$

where $\langle P_1 \rangle$ is average power of 1-γ excitation [photons/s], σ_1 is the 1-γ cross section [cm^2] of the chromophore, c is the concentration and L is the thickness of the sample [cm]. The detected 1-γ excited fluorescence is then:

$$F_1(t) = \Phi \eta \langle P_1 \rangle \sigma_1 cL \,. \tag{6}$$

Here, we assume that the fluorescence quantum yield, Φ, does not depend on the mode of excitation. This is reasonable, since, if Φ does not depend on the excitation wavelength then the same energy level does not have to be reached upon 1-γ and 2-γ excitation, so that the 1-γ wavelength does not have to be equal exactly to one half of the 2-γ wavelength. Then, by taking the ratio of the 1-γ and 2-γ fluorescence signals, the following expression for σ_2 is obtained:

$$\sigma_2 = \frac{F_2}{F_1} \frac{\lambda_2 f \tau \pi \langle P_1 \rangle \sigma_1 L}{4 g n \langle P_2 \rangle^2} . \tag{7}$$

The same mirrors and filters were used for 1-γ and 2-γ excitation (see Figure 2) to ensure that the fluorescence collection efficiency was the same in both cases. The single biggest source of error comes from the thickness of the demountable cell, which is known with 30% uncertainty. Hence, we assigned 30% error to the 2-γ cross section measurements. We used this method to measure σ_2 for Rhodamine B in methanol at 840 nm and Lucifer Yellow in water at 860 nm. The resulting values were 76 ± 23 GM (1 GM = 10^{-50} cm^4s/photon) and 2.8 ± 0.8 GM, respectively. Xu and Webb (17) reported a value of 210 GM for σ_2 of Rhodamine B. For Lucifer Yellow, they found the product $\sigma_2\Phi = 0.95$, where Φ is a quantum yield of fluorescence: taking $\Phi = 0.21$ (23), $\sigma_2 = 4.5$ GM. Hence, our values are lower than the published values for both compounds by a factor of about 2-3. However, for Rhodamine B at 802 nm, we measured $\sigma_2 = 60 \pm 18$ GM, while Oulianov *et al.* reported a value of 20.8 GM (24). Discrepancies of this magnitude are not unusual for 2-γ cross section measurements. For example, Kaatz and colleagues (25) compiled published 2-γ cross section values of several compounds measured around 1060 nm by different groups and found typical variations of a factor of 2 or 3: in particular, for Rhodamine B σ_2 varied between 4.6 and 13 GM. There is no simple explanation for these differences between experiments, other than the fact that many factors can potentially influence the measurements and result in unknown systematic errors that depend on the details of the experimental setup and technique used. We conclude, therefore, that our results below for Photofrin® are as accurate as the current state-of-the-art allows.

Two-photon PDT. YPEN-1 rat prostate endothelial cells were obtained from American type culture collection (ATCC, Manassas, VA, USA). These were grown in Eagle's Minimal Essential Medium F-15 (Gibco/Invitrogen, Burlington, ON, Canada) supplemented with 2 mM L-glutamine, 1.0 mM sodium pyruvate, 0.1 mM nonessential amino acids, 1.5 g/L sodium

bicarbonate and 5% heat-inactivated bovine calf serum (Hyclone, Logan, UT, USA). The cells were maintained at 37°C in a humidified atmosphere containing 5% CO_2/95% air.

For all experiments, cells were plated at 25% confluence in 2-well (4 cm^2 per well) chambered non-coated coverglass (Lab-Tek™ Chambered Coverglass, 1.0 Borosilicate coverglass, Nalge Nunc International, NY, USA). The final concentration of the cells before the irradiation was 10^6 cells/well. After growth for 26 h to allow attachment and doubling of the cell number, the media was replaced with media containing Photofrin at a concentration of 25 μg/ml. 24 h later cells were washed twice and replaced with CO_2-independent media (Gibco/Invitrogen, Burlington, ON, Canada) supplemented with 5% heat-inactivated bovine calf serum. The cells were then immediately placed under the 2-γ microscope and irradiated by the fs laser operating at 850 nm at an average power at the sample of 10 mW. The laser light was focused inside the cell layer so that Photofrin fluorescence was maximized and scanned over the cells as described above. A total of 800 scans were made. The total irradiation took approximately 800 seconds. The cells were then returned to the 37° C incubator in the dark and 3.5 h later were stained with Hoechst 33258 (10 μg/ml) and SYTOX Orange (2.5 μM) for 30 min. To relocate the irradiated region, the bottom of the well was marked with a diamond marker before irradiation. The fluorescence of the both stains was excited by means of 2-γ excitation at 800 nm and 10 mW. Any possible 2-γ PDT effect from this excitation is negligible because the process of image acquisition takes only about one minutes. The damage to the cells was estimated as ratio of the area cleared of cells to the total irradiated area.

RESULTS AND DISCUSSION

2-γ spectrum and cross section

Since, as expected (26), the Photofrin fluorescence signal was found to be higher in methanol than in water and this simplified the measurements, all 2-γ measurements except those *in vitro* were done in methanol solution. Figure 4a shows examples of the fluorescence as a function of the excitation power at two different excitation wavelengths, while Figure 4b shows the slope of the linear fits to each such curve as a function of excitation wavelength. For 1-γ interactions the absorption (as measured by the fluorescence signal) should be proportional to excitation power, while the dependence should be quadratic for 2-γ excitation. Figure 4b demonstrates that 2-γ absorption is the dominant mode of excitation above about 800 nm for Photofrin. The maximum of the last 1-γ absorption band of Photofrin in methanol is situated at 624 nm, but the probability of 1-γ absorption remains significant for wavelengths considerably greater than this wavelength. This is similar to the findings of Drobizhev *et al.* (27) for meso-tetra-alkynyl-porphyrins and is due to 1-γ absorption of molecules in thermally populated vibronic levels. It is important to establish directly from the excitation power dependence the spectral region where 2-γ dominates over 1-γ absorption, since the qualitative separation of the two spectral regions can be very misleading. Figure 5 presents the 2-γ spectrum of Photofrin in the range 800-900 nm, where the 1-γ contribution is negligible. The spectral profile decreases monotonically with increasing wavelength in this range, as has been reported for other porphyrins (28). This may represent the tail of a strong 2-γ transition situated at a shorter wavelength and/or resonance enhancement from nearby linear absorption bands.

In order to measure the 2-γ cross section the value of the 1-γ cross section is required at the wavelength used for 1-γ excitation, 488 nm (see Equation 7). The 1-γ cross section of Photofrin is difficult to define exactly since it comprises multiple porphyrin species whose relative concentrations vary with the exact conditions (29). Hence, we used a representative average value of 3200 $M^{-1}cm^{-1}$ at the peak of the 630 nm absorption band (29) to calculate the extinction coefficient at 488 nm. In this respect the 2-γ cross section can be considered as being averaged over the different Photofrin constituents. The 2-γ cross section measured at 850 nm was 7.4 ± 2.2 GM.

Table 1 presents 2-γ cross sections of several common 1-γ photosensitizers as well as some porphyrins and new potential 2-γ photosensitizers. The 2-γ cross section of the 1-γ photosensitizers ranges from 2 GM to 60 GM, demonstrating that Photofrin is typical in this respect. On the other hand, comparison to the porphyrin molecules shows that the 2-γ cross section of Photofrin is at the lower end of the possible values for porphyrins. The low 2-γ cross section of current 1-γ photosensitizers has stimulated the development of new 2-γ photosensitizers with greatly increased efficiency of 2-γ absorption. The 2-γ cross sections for some of these photosensitizers are presented in Table 1 for comparison. Two approaches that appear to be the most promising so far are based on modification of porphyrin molecules. In the first approach 2-γ chromophores are attached to the porphyrin macrocycle (13,15,16,37,39). The resulting cross section can be as high as 880 GM (15,37). The second approach is based on synthesizing conjugated porphyrin dimers (20,40), for which 2-γ cross sections can reach up to 10,000 GM due to double resonance effects (20). Singlet oxygen generation has been successfully demonstrated upon 2-γ excitation of both types of

photosensitizers (13,20,37,39). Clearly then, in terms of the photophysics, Photofrin as well as other 1-γ photosensitizers investigated so far are a relatively poor choice of 2-γ PDT agent. However, this must be balanced against other properties such as pharmacokinetics, microlocalization and toxicity.

2-γ PDT of endothelial cells

Figure 6 shows the 2-γ (a) and 1-γ (b) induced fluorescence of Photofrin in the same area of a YPEN-1 cell monolayer. The fluorescence pattern shows accumulation of the drug throughout the cytoplasm as has been observed previously (41). The fluorescence distribution in both images is virtually identical. Some of the areas in one of the images appear sharper than in the other one due to slightly different focusing depth of the lasers used for 1-γ and 2-γ excitation and cell movement between two modes of excitation. The similarity of the pictures confirms that Photofrin is excited upon 2-γ irradiation.

Figure 7 presents overlapped transmission and fluorescence images of 2-γ PDT-treated cells and controls 4 h after irradiation at a total exposure of 6300 Jcm^{-2}. The blue fluorescence comes from the Hoechst 33258 stain, which binds to DNA and stains nuclei. It is added to help visualize the cells. The red fluorescence comes from the vital stain SYTOX orange, which can only penetrate cells with compromised plasma membrane thus showing the dead cells. Both stains were added 3.5 h after irradiation. An excitation wavelength of 850 nm was used for treatment to exclude any possibility of 1-γ contributions (see Figure 4b). Figures 7(a,c,d) show three different regions of the cell monolayer treated with Photofrin and irradiated under the same conditions. Figure 7b shows the same region as Figure 7a with surrounding non-

irradiated region (note the different scale for 7b). Before treatment the cells formed a single continuous sheet at the bottom of the well so that the borders between cells were barely visible, while after treatment the cell monolayer was clearly disrupted.

Disruption of the cell monolayer and release of the cells from the substrate occurred during the four hour incubation following irradiation. Cellular morphology immediately following irradiation was virtually identical to control cells, but the cells slowly became rounder and appeared to shrink with a breakage of cell-cell contact followed by a loss of adherence to the substrate. Most of the irradiated cells died within four hours and subsequently detached from the surface of the well, leaving circular/oval empty regions in the middle of the irradiated area. Only small fraction of the dead cells remained attached to the surface, mostly around the border of the empty regions. There was some variability in the number of the dead cells as illustrated in Figures 7a, c, and d. This is possibly due to differences in the initial cell monolayer quality in the three irradiated regions.

Cell detachment resulted in circular/oval empty regions in the middle of the irradiated area (Figures 7a, c, and d). The 2-γ excited fluorescence of the Photofrin has the same intensity at the center and at the corners of the irradiated area (Figure 6a). Hence, the circular shape of the photodamaged region is not an experimental artifact due to uneven irradiation or drug uptake. Moreover, a similar effect is observed for 1-γ PDT with the argon-ion laser at 488 nm instead of the fs Ti:sapphire laser as the excitation source. 1-γ excitation is not as sensitive to the focusing of the laser light as 2-γ excitation, confirming again that this is a true biological response. One possible explanation is the minimization of “surface tension” at the cell monolayer boundary. For a given area, a circle has the smallest circumference. Therefore, the mechanical strain/surface tension on the cell membranes at the border of the empty region is

lowest for the circle, which may lead to the cells forming the rounded empty areas.

To estimate the fraction of the killed cells, we divided the area of the empty region by the total irradiated area. The resulting value was approximately 50%. Two types of controls were used to confirm that the observed cell response was due to 2-γ PDT. Firstly, cells without Photofrin were exposed to the same fs irradiation (Figure 7e) and, secondly, the fs laser was switched into CW mode at the same wavelength of 850 nm and cells with Photofrin were irradiated to the same total energy density (Figure 7f). Since the efficiency of 2-γ excitation by CW laser radiation is very low as compared to the fs laser radiation, no PDT effect is expected. Both controls show no effect on the cell layer, thus confirming that the cell layer destruction in Figure 7(a-d) is due to non-linear PDT.

The peak irradiance of the fs laser at the focal point can be very high, causing direct photodamage. However, we did not observe any damage to the control cells irradiated in the absence of Photofrin (Figure 7e) at the power settings used. Only when the average laser power was increased from 10 mW to above 30 mW at 850 nm did we observe damage from the fs pulses as illustrated in Figure 8. The cells destruction starts with what appears to be air bubbles formation. Note, that qualitatively this effect is different from what we observed during 2-γ PDT.

The average irradiance, *I*(*average*), at the focal point of the objective can be calculated according to the following expression (42):

$$I(average) = \frac{\pi \langle P \rangle}{2} \left(\frac{n}{\lambda} \right)^2 (1 - \cos\alpha)(3 + \cos\alpha), \quad (8)$$

where <*P*> is the average laser power after the objective, *n* is the refractive index of the immersion medium, λ is the wavelength and α is the semi-aperture angle of the objective

defined as $\alpha = \sin^{-1}(NA/n)$, where *NA* is a numerical aperture. Assuming a Gaussian pulse shape, the peak irradiance, *I*(*peak*), is then:

$$I(peak) = \left(\frac{\ln 2}{\pi}\right)^{1/2} \frac{2}{\tau f} I(average), \quad (9)$$

where τ and *f* are the pulse duration (FWHM) and repetition rate of the laser, respectively. The mechanical damage from fs radiation first appeared at around $P \approx 30$ mW, which corresponds to $8 \cdot 10^{11}$ Wcm^{-2}. This correlates well with the threshold peak irradiance of $6.8 \cdot 10^{11}$ Wcm^{-2} measured by König *et al.* (43) that caused morphological disruption of Chinese hamster ovary cells by 800 nm fs pulses (This peak irradiance was calculated using data in the published paper). From the point of view of 2-γ PDT, it is important that there is a power range at which 2-γ excitation of the photosensitizer can be efficiently performed while being below the cell culture damage threshold. Moreover, with new 2-γ photosensitizers (see Table 1), the required power of the fs lasers can be expected to be reduced even further.

We are aware of two other reports of 2-γ PDT treatments with Photofrin (12,44). In the work of König *et al.* (12), Chinese hamster ovary cells were incubated for 12 h in 5 μg/ml Photofrin and irradiated by 200 fs laser pulses at 780 nm (average power 2 mW, repetition rate 76 MHz, oil immersion objective 40×, NA1.3). The authors observed decreased cloning efficiency and loss of vitality after irradiation of the cells and attributed it to the 2-γ PDT effect. We note that there is some contribution of 1-γ absorption at this wavelength (see Figure 4b), so that the observed PDT effect may be due to both modes of excitation. In Wachter *et al.* (44) Photofrin (5 mg/kg body wt.) was administered via intraoperational injection into nude mice with subsequent irradiation (24 h later) of the liver by <200 fs laser pulses at 730 nm (repetition rate 76 MHz, objective and average power not stated). Acute massive necrosis was

observed in the irradiated area but, surprisingly, there was no effect using CW excitation at this wavelength, even although this excitation wavelength corresponds to the spectral region with almost pure 1-γ absorption (see Figure 4b). Thus, it is unlikely that the necrosis was due to 2-γ PDT.

Apart from Photofrin, several other photosensitizers have been investigated for their 2-γ PDT effects *in vitro* and *in vivo*. The first experiments in the 1980s employed nanosecond Nd:YAG lasers working at 1064 nm for 2-γ excitation and produced mixed results (45-47). Due to the low efficiency of 2-γ excitation by nanosecond pulses, the required light doses were high enough to cause hyperthermia, competing with possible PDT effects. Moreover, some studies failed to produce any significant 2-γ PDT effect at all (48,49). The use of fs Ti:sapphire lasers changed the situation by increasing the efficiency of 2-γ excitation and producing more reliable results. Aminolevulinic acid (ALA) in Chinese hamster ovary cells (12), 4'-aminomethyl-4,5,8-trimethylpsoralen in bacteria *Salmonella typhimurium* (11), hypocrellin A in HeLa cells (14), meso-tetra(hydroxyphenyl)-chlorin (mTHPC) in human colon carcinoma cells (50) and Chlorin-e_6-C_{15} monomethyl ester in liver cancer cells (35) were all shown to produce positive PDT responses upon their irradiation with fs (~10^2 fs) laser pulses around 800 nm.

Table 2 compares the experimental parameters used here for 2-γ PDT with typical 1-γ Photofrin-PDT values reported *in vitro* (see, e.g. reference 51). The excitation wavelength used in 2-γ PDT is mainly determined by the spectral region where 1-γ absorption by the photosensitizer is negligible and there are available ultrafast lasers, with Ti:sapphire laser being the most popular. Both conditions led to the use of near-IR wavelengths for 2-γ PDT, which matches well with the tissue transparency window. This is often presented as a basis for

2-γ PDT being advantageous for treating solid tumors, due to the greater penetration depth compared with shorter wavelengths typically used in 1-γ PDT. However, we are not aware of any direct experimental demonstration of this to date. Indeed, in highly scattering media such as tissue, 2-γ excitation at the beam focus is mainly due to ballistic photons, leading to fast degradation of the excitation efficiency with depth due to scattering (52). In addition, tissue absorption has larger effect on the efficiency of 2-γ excitation as compared to 1-γ excitation due to the quadratic dependence of the former on the light intensity. Hence, the main advantage of 2-γ PDT may rather be in its ability for highly targeted light delivery at or near the tissue surface. By tightly focusing the laser light, it is possible to limit 2-γ excitation and, correspondingly, the treatment volume to femtoliters, obviating damage even to the immediately adjacent (normal) tissue. This is particularly relevant for AMD since the neovasculature typically develops in the area responsible for central vision. Any damage to the surrounding healthy tissue can lead to significant decrease in visual acuity.

Ultrafast lasers with pulse durations ~ 10^2 fs and high instantaneous intensity are used for 2-γ PDT, while CW lasers (or non-laser sources) are typically used for 1-γ PDT. As discussed above, this difference is due to the strong dependence of the 2-γ efficiency on the instantaneous irradiance, I. With the interaction probabilities for 1-γ and 2-γ excitation being $P_1 = \sigma_1 I$ and $P_2 = \sigma_2 I^2/2$, where σ_1 and σ_2 are one- and two-photon cross sections, respectively, the relative probability of 2-γ excitation is:

$$\frac{P_2}{P_1} = \frac{\sigma_2 I}{2\sigma_1}. \qquad (10)$$

Using values typical for Photofrin, σ_1 = 3200 $M^{-1}cm^{-1} = 10^{-17}$ cm^2 and σ_2 = 10 GM = 10^{-49} cm^4s/photon, one can estimate, that if CW irradiation with I = 0.1 W/cm^2 ($4 \cdot 10^{17}$ photon/cm^2s)

is used for 2-γ excitation, then $P_2/P_1 \approx 2 \cdot 10^{-13}$, i.e. the 2-γ contribution is negligible under these conditions. On the other hand, with a fs laser, the instantaneous intensity is $2.6 \cdot 10^{11}$ Wcm^{-2} = $1 \cdot 10^{30}$ photons/cm^2s, yielding $P_2/P_1 \approx 5 \cdot 10^{-3}$. While the probability of 2-γ excitation is still two-three orders of magnitude lower than that of 1-γ, it is large enough for 2-γ PDT effects to be observed, as shown *in vitro* above.

Although fs lasers with pulse durations down to ~ 10 fs are commercially available, going much below 10^2 fs may be not desirable for 2-γ photon PDT. The first reason is the very strong dispersion of ultrashort pulses. This becomes particularly troublesome with pulse durations around 10 fs, for which propagation through the focusing optics and through the tissue lengthens the pulse duration to ~10^2 fs, thereby loosing any advantage of higher instantaneous intensity. It is possible to compensate for this effect by introducing negative dispersion before the laser pulse is launched into the optical system. Nevertheless, there is another more complex problem. Short laser pulses have broad a spectrum. A Gaussian Fourier transform limited laser pulse centered at 850 nm with a pulse duration of 10 fs has a spectral bandwidth (FWHM) of approximately 100 nm. With such a large bandwidth its spectrum may overlap with the 1-γ absorption spectrum of a photosensitizer. This will compromise the spatial selectivity achieved in pure 2-γ PDT.

The total fluence required for significant cell kill with Photofrin-PDT is several orders of magnitude larger for 2-γ than for 1-γ activation (6300 Jcm^{-2} vs. 10 Jcm^{-2}). This large difference is due to the very low value of σ_2 for Photofrin, resulting in two orders of magnitude lower probability of 2-γ excitation, as estimated above. In principal, the required fluence can be decreased by increasing laser power, because efficiency of 2-γ excitation

depends quadratically on laser power (Note that this is not true for 1-γ excitation). But we already operate at the power level close to the damage threshold by femtosecond laser pulses (see Figure 8). Hence, for 2-γ PDT to be practical, it will be necessary to use photosensitizers with σ_2 values that are 2 or 3 orders of magnitude higher than that of Photofrin, i.e. in the 10^3 GM range. New photosensitizers designed specifically to possess such high 2-γ cross sections are currently being developed and tested (see Table 1). Hence, if these have the other required properties (pharmacokinetics, microlocalization, toxicity, cost, etc.), it appears likely that the total fluence needed for significant photocytotoxicity will be clinically realistic.

CONCLUSIONS

The first main objective of the above studies was to establish and validate the technique for measuring the 2-γ absorption spectra and cross-sections of PDT sensitizers so as to ensure that there are negligible contributions from 1-γ interactions. The second objective was to establish and validate the use of an endothelial cell culture model, relevant in particular to vascularly-targeted treatments (either in tumors (53) or in AMD (3)), that can be used to demonstrate and quantify 2-γ PDT photocytotoxicity *in vitro*, again free of interference from 1-γ effects. Photofrin was used as a model photosensitizer, recognizing that it was never intended as an efficient 2-γ agent. The *in vitro* Photofrin-PDT dose response indicates that, unless novel irradiation procedures are used, it will be necessary to employ novel (or existing, but yet-to-be-identified) photosensitizers that have 2-γ cross-sections that are 2 or 3 orders of magnitude higher than that of Photofrin in the near-infrared. Such molecules indeed exist (Table 1) and are efficient singlet oxygen generators.

Based on such photosensitizers, we are collaborating on a multi-centre program to develop 2-γ PDT for treatment of AMD, in which the photophysical and *in vitro* methods described here are part of an evaluation platform for new 2-γ photosensitizers that also includes studies in a chick-embryo (CAM) model of neovasculature (54). In the near future, studies in rodent and rabbit models of choroidal neovasculature will be initiated, with imaging of the target tissue and delivery of the fs laser light for 2-γ PDT treatment via a confocal laser-scanning ophthalmoscope (55).

Acknowledgments. This work is part of a multi-institutional program supported by the Canadian

Institute for Photonic Innovations. Equipment was supported in part by the Canadian Foundation for Innovation and the Princess Margaret Hospital Foundation. The authors also thank Dr. Stuart Bisland and Mark Jarvi for providing us with Photofrin and YPEN-1 cells and James Jonkman for technical assistance with the 2-γ microscope.

REFERENCES

1. Dougherty T. J., C. J. Gomer, B. W. Henderson, G. Jori, D. Kessel, M. Korbelik, J. Moan, Q. Peng (1998) Photodynamic therapy. *J. Natl. Cancer Inst.* **90**, 889-905.
2. Wilson B. C. and M. S. Patterson (1986) The physics of photodynamic therapy. *Phys. Med. Biol.* **31**, 327-360.
3. Schmidt-Erfurth U. and T. Hasan (2000) Mechanisms of action of photodynamic therapy with verteporfin for the treatment of age-related macular degeneration. *Surv. Ophthalmol.* **45**, 195-214.
4. Vrouenraets M. B., G. W. M. Visser, G. B. Snow, G. A. M. S. van Dongen (2003) Basic principles, applications in oncology and improved selectivity of photodynamic therapy. *Anticancer Res.* **23**, 505-522.
5. Miller J. W. and E. S. Cragoudas (2004) Verteporfin PDT for experimental choroidal neovascularization. In *Photodynamic Therapy of Ocular Diseases.* (Edited by E. S. Gragoudas, J. W. Miller, L. Zografos), pp. 63-71. Lippincott Williams & Wilkins, Philadelphia, PA, USA.
6. Muller P. J. and B. C. Wilson (1995) Photodynamic therapy for recurrent supratentorial gliomas. *Semin. Surg. Oncol.* **11**, 345-354.
7. Denk W., J. H. Strickler, W. W. Webb (1990) Two-photon laser scanning fluorescence microscopy. *Science* **248**, 73-76.
8. Zipfel W. R., R. M. Williams, W. W. Webb (2003) Nonlinear magic: multiphoton microscopy in biosciences. *Nature Biotech.* **21**, 1369-1377.
9. Parrish J. A. (1981) New concepts in therapeutic photomedicine – photochemistry, optical

targeting and the therapeutic window. *J. Invest. Dermatol.* **77**, 45-50.

10. Bhawalkar J. D., N. D. Kumar, C.-F. Zhao, P. N. Prasad, (1997) Two-photon photodynamic therapy. *J. Clin. Lasers Med. Surg.* **15**, 201-204.
11. Fisher W. G., W. P. Partridge, Jr., C. Dees, E. A. Wachter (1997) Simultaneous two-photon activation of type-I photodynamic therapy agents. *Photochem. Photobiol.* **66**, 141-155.
12. König K., I. Riemann, P. Fischer (1999) Photodynamic therapy by nonresonant two-photon excitation. *Proc. SPIE* **3592**, 43-49.
13. Karotki A., M. Kruk, M. Drobizhev, A. Rebane, E. Nickel, C. W. Spangler (2001) Efficient singlet oxygen generation upon two-photon excitation of new porphyrin with enhanced nonlinear absorption. *IEEE J. Sel. Top. Quant. Electron.* **7**, 971-975.
14. Liu J., Y. W. Zhao, J. Q. Zhao, A. D. Xia, L. J. Jiang, S. Wu, L. Ma, Y. Q. Dong, Y. H. Gu (2002) Two-photon excitation studies of hypocrellins for photodynamic therapy. *J. Photochem. Photobiol. B* **68**, 156-164.
15. Spangler C. W., F. Meng, A. Gong, M. A. Drobizhev, A. Karotki, A. Rebane (2004) Nanophotonic ensembles for targeted multi-photon photodynamic therapy. *Proc. SPIE* **5331**, 84-91.
16. Oar M. A., J. A. Serin, W. R. Dichtel, J. M. J. Frechet (2005) Photosensitization of singlet oxygen via two-photon-excited fluorescence resonance energy transfer in a water-soluble dendrimer. *Chem. Mater.* **17**, 2267-2275.
17. Xu C. and W. W. Webb (1996) Measurement of two-photon excitation cross sections of molecular fluorophores with data from 690 to 1050 nm. *J. Opt. Soc. Am. B* **13**, 481-491.
18. Galanin M. D. and Z. A. Chizhikova (1966) Effective cross sections of 2-photon absorption in organic molecules. *JETP Lett.* **4**, 27-28.

19. Birge R. R., J. A. Bennett, B. M. Pierce, T. M. Thomas (1978) 2-photon spectroscopy of visual chromophores – evidence for a lowest excited $^1A_g^-$-like $\pi\pi^*$ state in *all-trans*-retinol (vitamin-A). *J. Am. Chem. Soc.* **100**, 1533-1539.

20. Hermann J. P. and J. Ducuing (1972) Absolute measurement of 2-photon cross-sections. *Phys. Rev. A* **5**, pp. 2557-2568.

21. Song J. M., T. Inoue, H. Kawazumi, T. Ogawa (1999) Determination of two photon absorption cross section of fluorescein using a mode locked titanium sapphire laser. *Anal. Sci.* **15**, 601-603.

22. Karotki A., M. Drobizhev, M. Kruk, C. Spangler, E. Nickel, N. Mamardashvili, A. Rebane (2003) Enhancement of two-photon absorption in tetrapyrrolic compounds. *J. Opt. Soc. Am. B* **20**, 321-332.

23. Stewart W. W. (1981) Synthesis of 3,6-disulfonated 4-aminonaphthalimides. *J. Am. Chem. Soc*. **103**, 7615-7620.

24. Oulianov D. A., I. V. Tomov, A. S. Dvornikov, P. M. Rentzepis (2001) Observations on the measurement of two-photon absorption cross-section. *Opt. Comm.* **191**, 235-243.

25. Kaatz P. and D. P. Shelton (1999) Two-photon fluorescence cross-section measurements calibrated with hyper-Rayleigh scattering. *J. Opt. Soc. Am. B* **16**, 998-1006.

26. Andreoni A. and R. Cubeddu (1984) Photophysical properties of Photofrin II in different solvents. *Chem. Phys. Lett.* **108**, 141-144.

27. Drobizhev M., A. Karotki, M. Kruk, A. Krivokapic, H. L. Anderson, A. Rebane (2003) Photon energy upconversion in porphyrins: one-photon hot-band absorption versus two-photon absorption. *Chem. Phys. Lett.* **370**, 690-699.

28. Drobizhev M., A. Karotki, M. Kruk, A. Rebane (2002) Resonance enhancement of two-

photon absorption in porphyrins. *Chem. Phys. Lett.* **355**,175-182.

29. Jori G. (1996) Tumor photosensitizers: approaches to enhance the selectivity and efficiency of photodynamic therapy. *J. Photochem. Photobiol. B* **36**, 87-93.
30. Bodaness R. S., D. F. Heller, J. Krasinski, D. S. King (1986) The two-photon laser-induced fluorescence of the tumor-localizing photosensitizer hematoporphyrin derivative. Resonance-enhanced 750 nm two-photon excitation into the near-UV Soret band. *J. Biol. Chem.* **261**, 12098-12101.
31. Oh D. H., R. J. Stanley, M. Lin, W. K. Hoeffler, S. G. Boxer, M. W. Berns, E. A. Bauer (1997) Two-photon excitation of 4'-hydroxymethyl-4,5',8-trimethylpsoralen. *Photochem. Photobiol.* **65**, 91-95.
32. Meshalkin Y. P., E. E. Alfimov, N. E. Vasil'ev, A. N. Denisov, V. K. Makukha, A. P. Ogirenko (1999) Two-photon excitation of aluminium phthalocyanines. *Quant. Electron.* **29**, 1066-1068.
33. Goyan R. L. and D. T. Cramb (2000) Near-infrared two-photon excitation of protoporphyrin IX: photodynamics and photoproduct generation. *Photochem. Photobiol.* **72**, 821-827.
34. Kruk M.**,** A. Karotki, M. Drobizhev, A. Rebane, G. Isakov, P. Petrov (2003) Two-photon excitation in photodynamic therapy. Proceedings of the International Conference *Laser Physics and Applications*. (Edited by N. S. Kazak, V. A. Savva, A. P. Nizovtsev, G. R. Mostovnikova), Minsk, pp.263-265.
35. Chen P., P. D. Zhao, P. Guo, L. Lin, J. W. Liu, Q. Yu (2005) Two-photon excitation of Chlorin-e_6-C_{15} Monomethyl Ester for photodynamic therapy. *Proc. SPIE* **5630**, 209-217.
36. Drobizhev M., A. Karotki, M. Kruk, N. Zh. Mamardashvili, A. Rebane (2002) Drastic enhancement of two-photon absorption in porphyrins associated with symmetrical electron-

accepting substitution. *Chem. Phys. Lett.* **361**, 504-512.

37. Drobizhev M., A. Karotki, M. Kruk, Y. Dzenis, A. Rebane, F. Meng, C. W. Spangler (2003) Strong two-photon absorption in new porphyrins with asymmetrical *meso*-substitution. *Proc. SPIE* **5211**, 63-74.
38. Drobizhev M., Y. Stepanenko, Y. Dzenis, A. Karotki, A. Rebane, P. N. Taylor, H. L. Anderson (2004) Extremely strong near-IR two-photon absorption in conjugated porphyrin dimers: quantitative description with three-essential-states model. *J. Phys. Chem. B* **109**, 7223-7236.
39. Dichtel W. R., J. M. Serin, C. Edder, J. M. J. Frechet, M. Matuszewski, L. S. Tan, T. Y. Ohulchanskyy, P. N. Prasad (2004) Singlet oxygen generation via two-photon excited FRET. *J. Am. Chem. Soc.* **126**, 5380-5381.
40. Ogawa K., A. Ohashi, Y. Kobuke, K. Kamada, K. Ohta (2003) Strong two-photon absorption of self-assembled butadiene-linked bisporphyrin. *J. Am. Chem. Soc.* **125**, 13356-13357.
41. Wilson B. C., M. Olivo, G. Singh (1997) Subcellular localization of Photofrin® and aminolevulinic acid and photodynamic cross-resistance *in vitro* in radiation-induced fibrosarcoma cells sensitive or resistant to Photofrin-mediated photodynamic therapy. *Photochem. Photobiol.* **65**, 166-176.
42. Cogswell C. J. and K. G. Larkin (1995) The specimen illumination path and its effect on image quality. In *Handbook of Biological Confocal Microscopy.* (Edited by J. B. Pawley), pp. 127-137. Plenum Press, New York.
43. König K., P. T. C. So, W. W. Mantulin, B. J. Tromberg, E. Gratton (1996) Two-photon excited lifetime imaging of autofluorescence in cells during UVA and NIR photostress. *J. Miscrosc.* **183**, 197-204.

44. Wachter E. A., M. G. Petersen, H. C. Dees (1999) Photodynamic therapy with ultrafast lasers. *Proc. SPIE* **3616**, 66-74.

45. Inaba H., M. Shimamoto, S. Mashiko, S. Sato, T. Kuwahara, Y. Taguchi, M. Kasai (1985) Nd:YAG laser-induced hematoporphyrin visible fluorescence and two-photon-excited photochemical effect on malignant tumor cells. *J. Opt. Soc. Am. A* **2**, P72.

46. Mashiko S., S. Sato, H. Inaba, M. Kasai, S. Kimura (1986) Two-photon excited visible fluorescence of hematoporphyrin and pheophorbide *a* and *in vitro* experiments of the photodynamic effect on cultured cancer cells using a Nd:YAG laser. *J. Opt. Soc. Am. B* **3**, P72-P73.

47. Fujishima I., T. Sakai, Y. Fijishima, H. Ryu, K. Uemura, N. Daikuzono, T. Yamane, S. Watanabe (1987) Experimental studies of photodynamic therapy and laser hyperthermia in brain tumor using Nd:YAG laser and pheophorbide-a. *Lasers Surg. Med.* **7**, 104-105.

48. Marchesini R., E. Melloni, G. Pezzoni, G. Savi, F. Zunino, F. Docchio, G. Fava (1986) A study on the possible involvement of nonlinear mechanism of light absorption by HpD with Nd:YAG laser. *Lasers Surg. Med.* **6**, 323-327.

49. Lenz P. (1995) *In vivo* excitation of photosensitizers by infrared light. *Photochem. Photobiol.* **62**, 333-338.

50. Schneider M., G. Graschew, T. A. Roelofs, E. Balanos, S. Rakowsky, H. J. Sinn, P. M. Schlag (2000) Multiphoton excitation and photodynamic activity of macromolecular derivatized mTHPC. *Proc. SPIE* **3909**, 60-65.

51. Chang C.-J., C.-H. Sun, L.-H. L. Liaw, M. W. Berns, J. S. Nelson (1999) In vitro and in vivo photosensitizing capabilities of 5-ALA versus Photofrin in vascular endothelial cells. *Lasers Surg. Med.* **24**, 178-186.

52. Karlsson D. and H. Nilsson (2001) A study of two-photon excitation in turbid media – possibilities in photodynamic therapy. *Master's Thesis*, Lund University, Lund, Sweden (http://www-atom.fysik.lth.se/REPRINTS/LRAP-277/LRAP-277Abstract.asp).

53. Krammer B (2001) Vascular Effects of Photodynamic Therapy. *Anticancer Res.* **21**, 4271-4278.

54. Samkoe K. S. and D. T. Cramb (2003) Application of an *ex ovo* chicken chorioallantoic membrane model for two-photon excitation photodynamic therapy of age-related macular degeneration. *J. Biomed. Opt.* **8**, 410-417.

55. Roorda A, F. Romero-Borja, W. J. Donnelly, H. Queener, T. J. Hebert, M. C. W. Campbell (2002) Adaptive optics scanning laser ophthalmoscopy. *Opt. Express* **10**, 405-412.

FIGURE LEGENDS

Figure 1. (a) Energy level diagram for PDT, based on Type-II photochemistry. The singlet-excited states may be populated either by absorption of a single photon (1-γ PDT) or by simultaneous absorption of 2 photons (2-γ PDT), each of half the energy (double the wavelength) of the single photon required to excite the same transition. After internal conversion to the first excited singlet level the photophysical and photochemical processes are identical for 1-γ and 2-γ PDT. (b) Three-dimensional localization of the 2-γ effect that can be used for high precision PDT treatment. The pictures on the left and right show 1-γ and 2-γ excited fluorescence of Rhodamine B, respectively. The 1-γ fluorescence is excited by a CW argon-ion laser at 488 nm. The 2-γ fluorescence is excited by a femtosecond Ti:sapphire laser at 840 nm. The excitation laser light is focused by 5×/NA0.25 objective into the solution with Rhodamine B. 1-γ fluorescence is visible throughout the beam depth while 2-γ fluorescence is localized at the focal point.

Figure 2. Schematic diagram of the excitation (solid) and fluorescence collection (dashed) pathways of the microscope. HFT KP 700/488 is a mirror reflecting at 488 nm and above 700 nm. NFT is a long pass 490 nm filter. Following bandpass (BP) filters are used: BP 535-590 (Lucifer Yellow), BP 565-615 (Rhodamine B, SYTOX Orange), BP 650-710 (Photofrin) and BP 435-485 (Hoechst 33258). PMT is a photomultiplier. A fs Ti:sapphire laser was used for 2-γ excitation and argon-ion laser was used for 1-γ excitation. An objective 10×, NA = 0.5 was used for 2-γ spectral and cross section measurements and objective 40×, NA = 1.2 (water immersion), was used for 2-γ PDT experiments.

Figure 3. 2-γ spectrum of Rhodamine B in methanol measured relative to Lucifer Yellow in water. Solid squares – spectrum measured in this work. Open circles – spectrum measured directly from ref (17). Both data sets are normalized to unity at the maximum. The insert shows a double logarithm plot of the 2-γ excited fluorescence intensity as a function of the excitation power for Lucifer Yellow (squares) and Rhodamine B (triangles). The excitation wavelength was 800 nm. Black lines are best linear fits.

Figure 4. (a) Double logarithm plot of the Photofrin (100 μg/ml in methanol) fluorescence intensity versus the excitation power at 750 nm (squares) and 850 nm (triangles). While there are contributions from both 1-γ and 2-γ excitation at 750 nm, the plot appears linear because the power range is not large enough to produce significant deviation from linearity. (b) Resulting slope as a function of the excitation wavelength: pure 2-γ excitation starts above 800 nm.

Figure 5. 2-γ absorption spectrum (■) of Photofrin in methanol. Also shown is the 1-γ absorption spectrum scaled to the 2-γ cross section at 850 nm.

Figure 6. Photofrin fluorescence images of the same area of a YPEN-1 cell monolayer after 24 h incubation in 25 μg/ml Photofrin. (a) 2-γ excited fluorescence, excitation wavelength 850 nm; (b) 1-γ excited fluorescence, excitation wavelength 488 nm. The scale bar is 20 μm.

Figure 7. Overlapped fluorescence and transmission images showing the effect of 2-γ Photofrin-PDT on YPEN-1 rat prostate endothelial cells 4 h after treatment (Photofrin concentration 25 μg/ml, incubation time 24 h, excitation wavelength 850 nm, average power 10 mW, 800 scans, 6300 Jcm^{-2}). The blue fluorescence comes from Hoechst 33258, which stains both, dead and alive cells and is added to simplify the visualization of the cell monolayer. The red fluorescence comes from the vital stain SYTOX Orange, which stains only cells with compromised plasma membrane. Both stains were added 3.5 h after irradiation 30 min before the images were acquired. (a,c,d) three different regions of a cell monolayer treated with 2-γ PDT, b) the same as for (a) but including the adjacent non-irradiated region, the irradiated area is inside of the white square, e) control cells without Photofrin irradiated by fs laser light, f) control cells with Photofrin irradiated by Ti:sapphire laser working in CW mode. The scale bar is equal to 20 μm for (a, c-f) and 50 μm for (b). The number of cells in (f) is smaller because initial cell density in the cell monolayer is smaller.

Figure 8. Damage to the cell monolayer (no Photofrin) induced by a fs laser operating at 850 nm, 40 mW average power. The scale bar is 20 μm. (a) cell monolayer before irradiation. (b) cell monolayer after 400 scans. (c) cell monolayer after 800 scans.

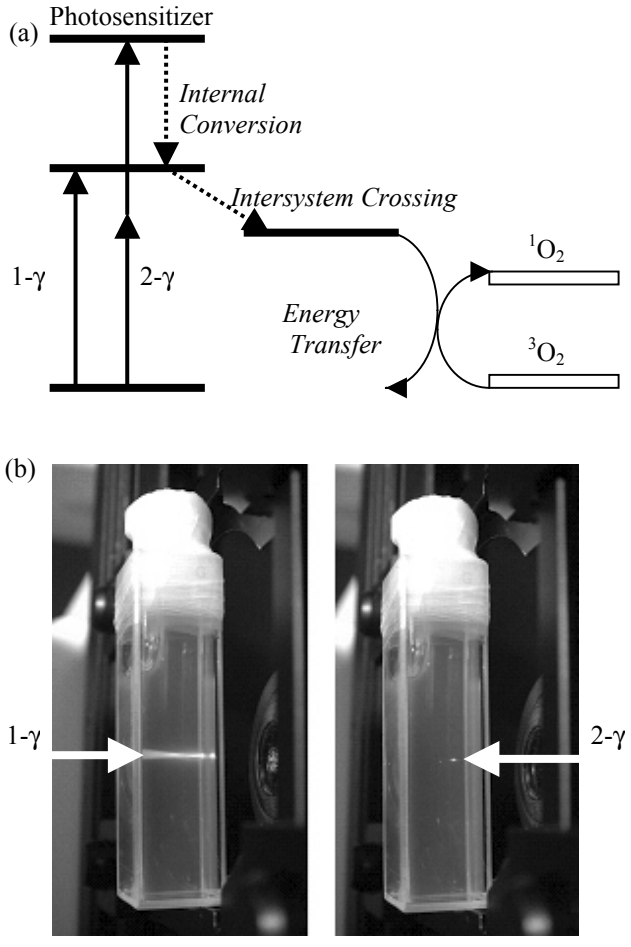
(a)
Photosensitizer
Internal
Conversion
Intersystem Crossing
1-γ
2-γ
Energy
Transfer
$^1O_2$
$^3O_2$
(b)
1-γ
2-γ

Figure 1

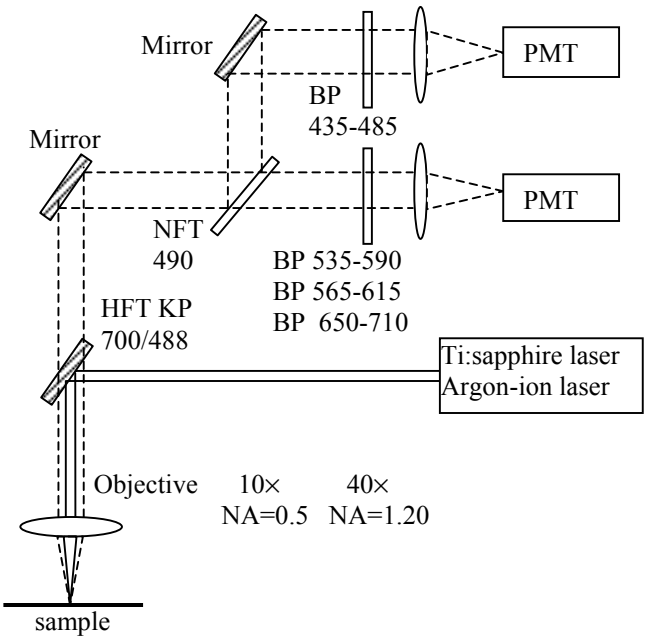
Mirror
PMT
BP
435-485
Mirror
PMT
NFT
490
BP 535-590
BP 565-615
BP 650-710
HFT KP
700/488
Ti:sapphire laser
Argon-ion laser
Objective
10×
NA=0.5
40×
NA=1.20
sample

Figure 2

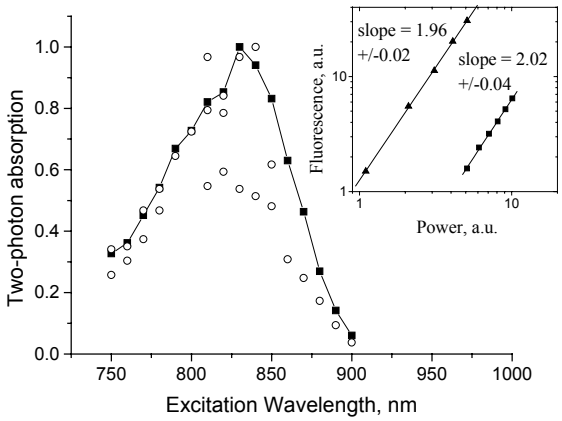
Two-photon absorption
Excitation Wavelength, nm
slope = 1.96
+/-0.02
slope = 2.02
+/-0.04
Fluorescence, a.u.
Power, a.u.

Figure 3

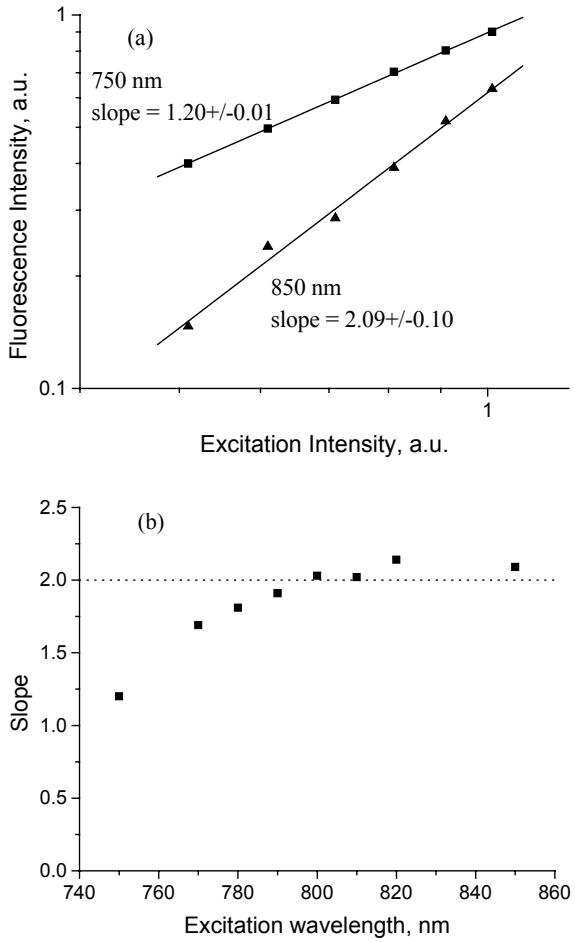
(a)
750 nm
slope = 1.20+/-0.01
850 nm
slope = 2.09+/-0.10
Fluorescence Intensity, a.u.
Excitation Intensity, a.u.
1
0.1
1
(b)
Slope
Excitation wavelength, nm
2.5
2.0
1.5
1.0
0.5
0.0
740
760
780
800
820
840
860

Figure 4

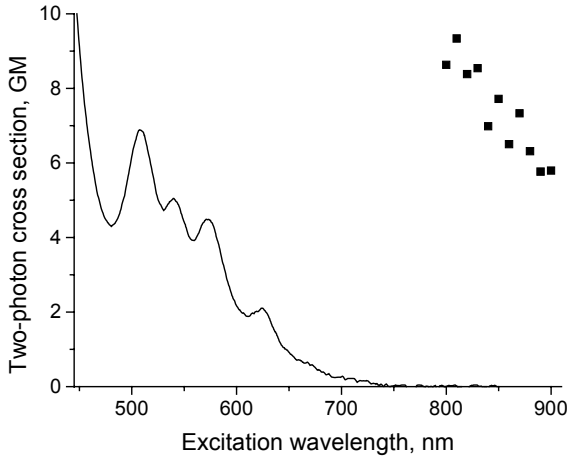
Two-photon cross section, GM
Excitation wavelength, nm
0
2
4
6
8
10
500
600
700
800
900

Figure 5

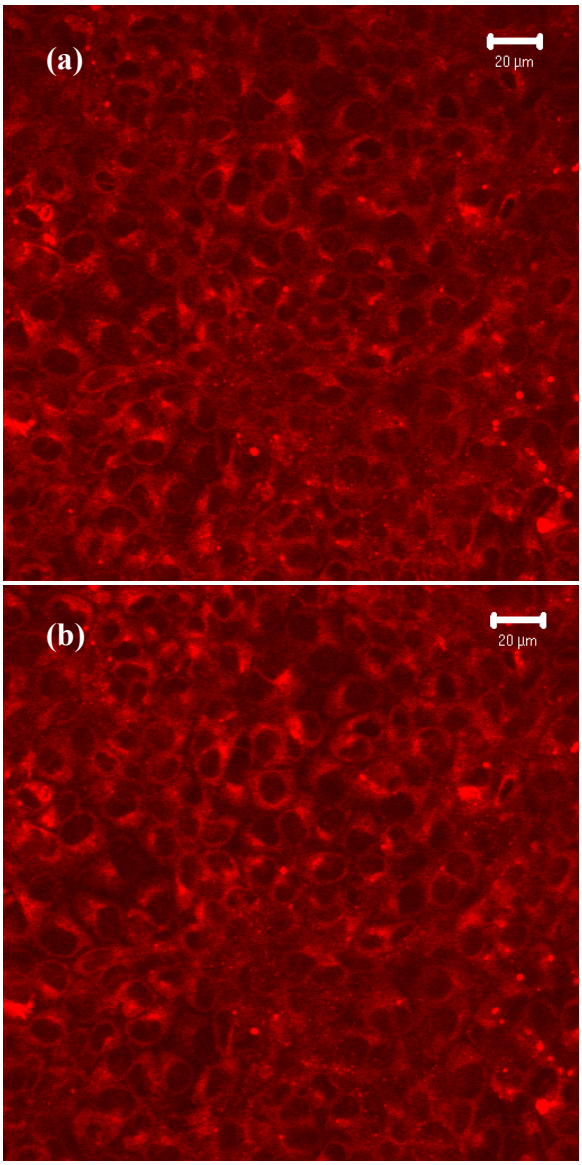

Figure 6

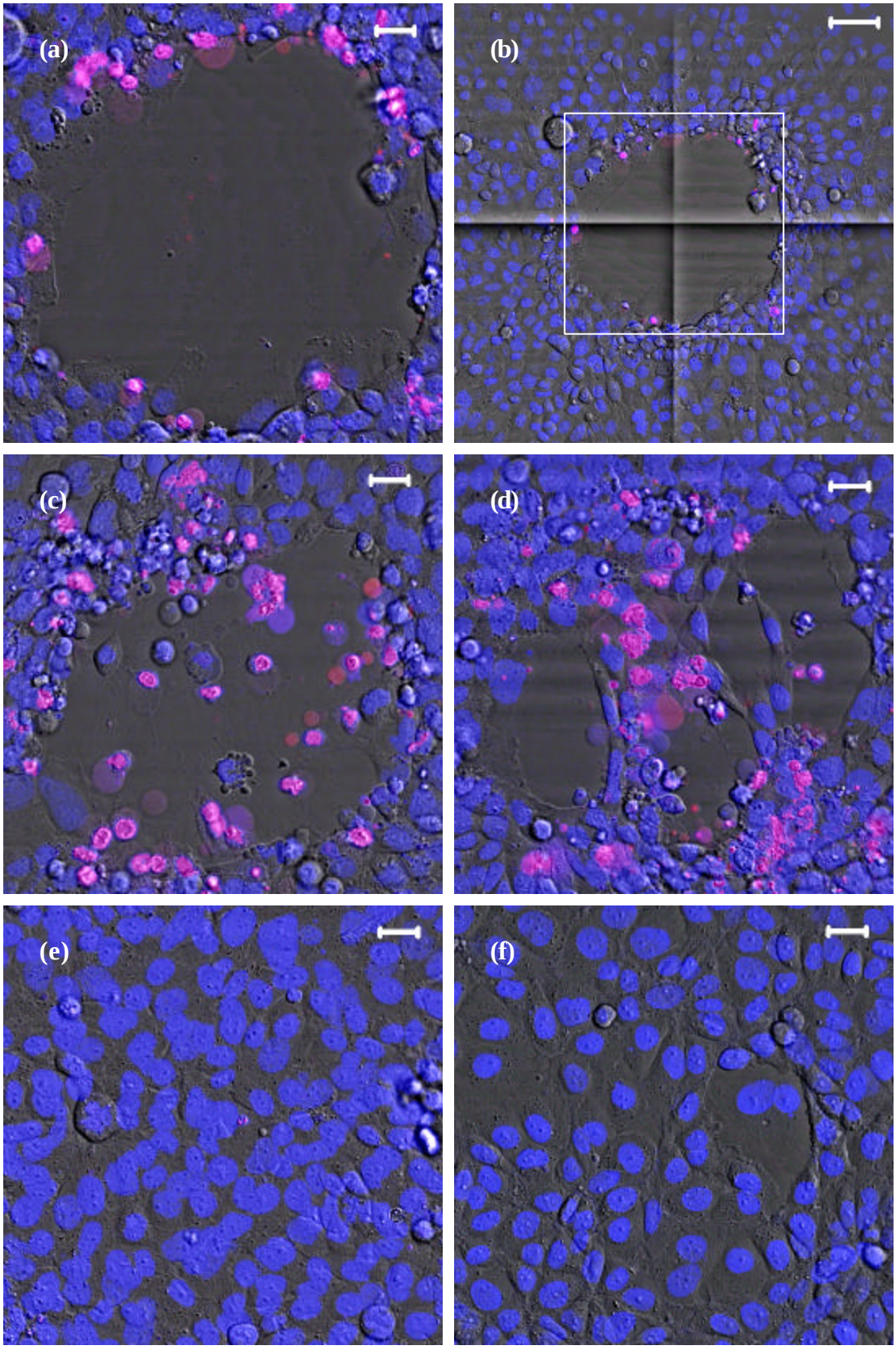

Figure 7

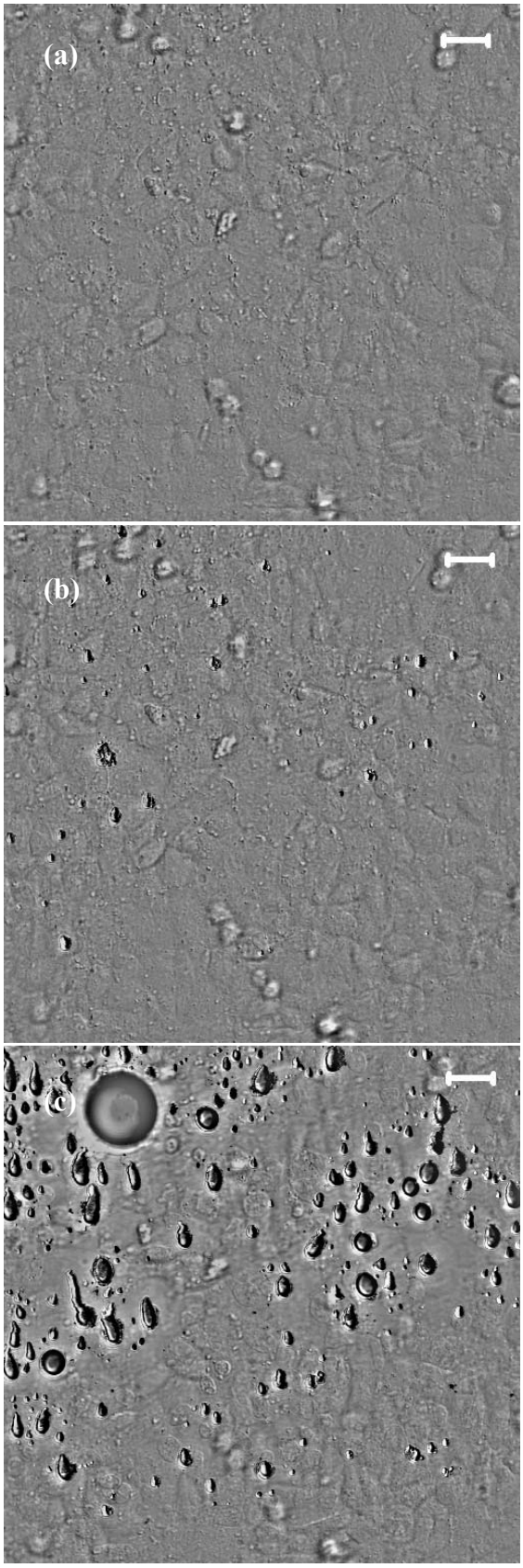

Figure 8

Table 1. 2-γ cross sections of common 1-γ photosensitizers, porphyrin molecules and new 2-γ photosensitizers.

	σ_2, GM	Wavelength, nm	
Photofrin®	**7.4**	**850**	
HPD[†] (30)	15	750	common 1-γ
HMT[‡] (31)	20	730	photosensitizers
Al-phthalocyanine (32)	12.7	1064	
Photosens (32)	5[§]	1064	
Protoporphyrin IX (33)	2	790	
Hypocrellin A (14)	34.8	800	
Hypocrellin B (14)	21.3	800	
Photolon (34)	60	800	
Chlorin-e_6[‖] (35)	29.1	800	
ZnOEP (28)	4.4	780	porphyrins
H_2TPP (28)	15	780	
H_2TBP (28)	20	780	
ZnMPTBP (28)	67	780	
ZnDiPTBP (28)	50	780	
ZnTriPTBP (28)	130	780	
ZnTPTBP (28)	90	780	
Bu_4TAP (36)	70	783	
$(BrPh)_8$TAP (36)	380	802	
$(NO_2Ph)_8$TAP (36)	900	802	
Porphyrin+stilbene (15, 37)[¶]	110 – 880	795	new 2-γ
Porphryin dimers (38)[††]	3100 - 10100	825 - 875	photosensitizers

[†]Hematoporphyrin derivative

[‡]4’-hydroxymethyl-4,5’,8-trimethylpsoralen

[§]Product of the 2-γ cross section and fluorescence quantum yield

[‖]Chlorin-e_6-C_{15} monomethyl ester

[¶]The porphyrin macrocycle is *meso*-substituted with stilbene-based substituents. The 2-γ cross section was measured for porphyrins with 6 different substituents and varied between 110 and 880 GM.

[††]Conjugated porphyrin dimers. The TPE spectra were measured for 6 different dimers for which the maximum value of σ_2 varied between 3,100 and 10,100 GM at peak wavelengths of 825-875 nm.

Table 2. Irradiation parameters used for 2-γ Photofrin-PDT in this work and typical for 1-γ Photofrin-PDT (see, e.g. reference 51) *in vitro*.

	2-γ	1-γ
Wavelength (nm)	850	630
Pulse duration (fs)	300	CW
Repetition rate (MHz)	90	N/A
Average irradiance (Wcm^{-2})	7.5×10^{6}	~0.1
Peak irradiance (Wcm^{-2})	2.6×10^{11}	~0.1
Fluence (Jcm^{-2})	6300	~10